

Downregulation of EphB2 by RNA interference attenuates glial/fibrotic scar formation and promotes axon growth

<https://doi.org/10.4103/1673-5374.317988>

Jian Wu, Zhen-Yu Zhu, Zhi-Wei Fan, Ying Chen, Ri-Yun Yang, Yi Li*

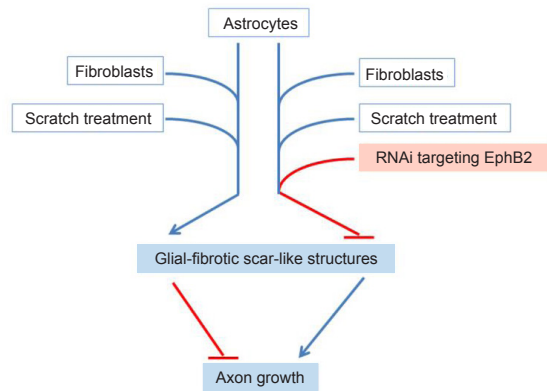
Date of submission: September 15, 2020

Date of decision: March 25, 2021

Date of acceptance: May 10, 2021

Date of web publication: July 8, 2021

Graphical Abstract Downregulation of EphB2 by RNA interference attenuates glial/fibrotic scar formation and promotes axon growth



Abstract

The rapid formation of a glial/fibrotic scar is one of the main factors hampering axon growth after spinal cord injury. The bidirectional EphB2/ephrin-B2 signaling of the fibroblast-astrocyte contact-dependent interaction is a trigger for glial/fibrotic scar formation. In the present study, a new in vitro model was produced by coculture of fibroblasts and astrocytes wounded by scratching to mimic glial/fibrotic scar-like structures using an improved slide system. After treatment with RNAi to downregulate EphB2, changes in glial/fibrotic scar formation and the growth of VSC4.1 motoneuron axons were examined. Following RNAi treatment, fibroblasts and astrocytes dispersed without forming a glial/fibrotic scar-like structure. Furthermore, the expression levels of neurocan, NG2 and collagen I in the coculture were reduced, and the growth of VSC4.1 motoneuron axons was enhanced. These findings suggest that suppression of EphB2 expression by RNAi attenuates the formation of a glial/fibrotic scar and promotes axon growth. This study was approved by the Laboratory Animal Ethics Committee of Jiangsu Province, China (approval No. 2019-0506-002) on May 6, 2019.

Key Words: astrocyte; EphB2; fibroblast; glial/fibrotic scar; microfluidic platform; RNAi; spinal cord injury; VSC4.1 motoneuron

Chinese Library Classification No. R456; R741; Q789

Introduction

After spinal cord injury (SCI), death of spinal neurons and shearing of axons can result in the loss of sensory and motor functions, dysfunction of multiple systems, and even chronic neuropathic pain. However, effective pathology-modifying and regenerative treatments are still lacking. One cardinal obstacle to recovery from SCI is the inhospitable microenvironment, especially the rapid formation of a glial/fibrotic scar at the site of injury (Orr and Gensel, 2018; Tran et al., 2018), which not only acts as a mechanical barrier, but also secretes extracellular matrix (ECM) components that inhibit the growth of axons (Sofroniew, 2018). Among ECMs, chondroitin sulfate proteoglycans (CSPGs) are the major component (Rosenzweig et al., 2019; Hussein et al., 2020; Sami et al.,

2020). Accordingly, recent studies have focused on methods to eliminate the glial/fibrotic scar; however, the impact on the growth of axons has been limited (Karimi-Abdolrezaee et al., 2010; Tran and Silver, 2015; Choi et al., 2021; Zhou et al., 2021). Thus, strategies that prevent scar formation might be more fruitful than interventions post scar formation.

Recent studies have shown that both EphB2 and ephrin-B2 participate in the formation of the glial/fibrotic scar (Ren et al., 2013; Yang et al., 2018; Dun and Parkinson, 2020). In the early stages of SCI, EphB2 and ephrin-B2 are upregulated in meningeal fibroblasts and astrocytes, respectively (Bundesen et al., 2003; Li et al., 2017). Contact between these two types of migrating cells enables specific EphB2/ephrin-B2 binding, which triggers a bidirectional signaling cascade in both cell

Department of Histology and Embryology, Medical College, Nantong University, Nantong, Jiangsu Province, China

*Correspondence to: Yi Li, PhD, ly1203@ntu.edu.cn.

<https://orcid.org/0000-0002-7497-4823> (Yi Li)

Funding: This work was supported by the Priority Academic Program Development of Jiangsu Higher Education Institutes of China (PAPD); the Science and Technology Plan Project of Nantong of China, No. JC2020026 (to JW); the National Science Research of Jiangsu Higher Education Institutes of China, No. 19KJB310012 (to RYY)

How to cite this article: Wu J, Zhu ZY, Fan ZW, Chen Y, Yang RY, Li Y (2022) Downregulation of EphB2 by RNA interference attenuates glial/fibrotic scar formation and promotes axon growth. *Neural Regen Res* 17(2):362-369.

types, causing them to gather at the edge of the injury site and for ECM components to accumulate in the intercellular spaces. The glial/fibrotic scar is formed 2 weeks after SCI, and the upregulation of EphB2 and ephrin-B2 is the initial and key step in its formation (Bundesen et al., 2003; Goldshmit et al., 2006; Sofroniew, 2009; Taylor et al., 2017). Based on this information, we hypothesized that specific inhibition of the expression of EphB2 or ephrin-B2 may hinder the formation of a glial/fibrotic scar in the early stages. Furthermore, RNA interference (RNAi), which is widely used in basic research and many clinical treatments (Saw and Song, 2020; Donia and Bokhari, 2021), can be used to downregulate EphB2 and/or ephrin-B2, thereby inhibiting the formation of the glial/fibrotic scar and reducing its negative effects, as well as limiting the expansion of damage and repairing the blood-brain barrier (Schachtrup et al., 2010).

It is worth noting that most neuronal somata of damaged axons are distant from the site of injury in SCI. When studying the response of axons to changes in the surrounding microenvironment under traditional cell culture conditions, it is impossible to isolate the axon from the cell body. To resolve this issue, a microfluidic platform has been created in which the neuronal somata can be cultured in a chamber capable of emitting microchannels, and neuronal axons grow into adjacent chambers through these microchannels so that the somata and axons are separated in space (Li et al., 2017; Wang et al., 2018). Additionally, there is a unique microfluidic force between the chambers at different liquid levels, which allows the fluid to flow into the microchannels and connect the chambers in only one direction. Therefore, molecules that are downstream will not contaminate those that are upstream (Yang et al., 2009, 2015). A specific difference in chemical composition between the two chambers is created, and this technique has become an exceptional tool in neurobiology research (Millet and Gillette, 2012; Park et al., 2013).

In the present study, we used a new *in vitro* glial/fibrotic scar model and used RNAi to specifically downregulate the expression of EphB2. We then reduced the binding of EphB2 to its cognate ligand to partially inhibit the formation of the glial/fibrotic scar. Additionally, we designed a microfluidic platform suitable for this experiment and used it to assess the effect of small interfering RNA (siRNA) targeting EphB2 on the growth of spinal motoneuron axons.

Materials and Methods

Cell culture

Primary fibroblasts and astrocytes were cultured from 60 postnatal day (P) 1 Sprague-Dawley rats (specific-pathogen-free grade) from the Laboratory Animal Center of Nantong University in China (license No. SYXK (Su) 2017-0046) using a variation of the procedure described by Kimura-Kuroda et al. (2010). The experiments were approved by the Laboratory Animal Ethics Committee of Jiangsu Province, China (approval No. 2019-0506-002) on May 6, 2019. Briefly, fibroblasts and astrocytes were taken from spinal cords of rats after neonates were euthanized with carbon dioxide (Shomer et al., 2020). The CO₂ displacement rate is 30–70%, which ensures that the rats have lost consciousness before causing pain. The intervention time of CO₂ was 35 minutes. Spinal cord meninges were digested in 0.125% trypsin-ethylenediaminetetraacetic acid (Gibco, Gaithersburg, MD, USA) for 18 minutes, plated in 75-cm² flasks (Corning, New York, NY, USA) precoated with poly-L-lysine (Gibco), and cultured in Dulbecco's modified Eagle medium/F12 (DMEM/F12) (Gibco), supplemented with 10% fetal bovine serum (FBS) (Gibco) and 1% (v/v) penicillin-streptomycin (Gibco).

After the meninges were removed, the spinal cords were digested in 0.125% trypsin-ethylenediaminetetraacetic acid (Gibco) for 12 minutes, plated in 75-cm² flasks (Corning), and

cultured in the same medium as above. When confluence was reached to 90%, the flasks were shaken at 280 r/min for 18 hours. After the suspension was removed, the remaining cells were digested again and cultured in clean flasks (Corning).

VSC4.1 motoneurons were provided as a gift by Baylor College of Medicine (Houston, TX, USA). These cells are derived from a fusion of the ventral neuron of an embryonic rat spinal cord with the mouse N18TG2 neuroblastoma cell line (Chakrabarti et al., 2014; Ferguson and Subramanian, 2016), and are used in studies of the CNS (Chakrabarti et al., 2014; Li et al., 2019). These cells proliferate in DMEM/F12 with 5% FBS and stick out processes in DMEM/F12 with 0.5% FBS.

The *in vitro* glial/fibrotic scar model

The improved slide system was modified from the Lab-Tek II chamber slide (Thermo Fisher Scientific, Waltham, MA, USA). The improved slide system consists of a bottom slide and an upper shelf with four chambers. Before use, the slide system was washed, sterilized, and precoated with poly-L-lysine. The upper shelf comprising the four chambers was removed from the Lab-Tek II chamber slide. Purified second to third passage fibroblasts and astrocytes were seeded at 6×10^4 and 8×10^4 cells/mL, respectively, in two adjacent chambers of the improved slide system (Figure 1A). After cell attachment, the upper shelf was removed, and the cells on the slides continued to be cultured with the same medium in 100-mm dishes (Corning). Three days later, the narrow space between the two types of cells disappeared, and different treatments were applied to the cells.

The astrocyte-fibroblast interactions at their interface is regarded as an indicator of scar observation (Abnet et al., 1991; Bundesen et al., 2003; Shearer et al., 2003). Our experiment included the following groups: (i) fibroblast/astrocyte coculture without any treatment, (ii) fibroblast/astrocyte coculture with only siRNA treatment, (iii) fibroblast/astrocyte coculture with scratch treatment using a 5-mL syringe needle at the interface between the two types of cells (one vertical scratch and twenty horizontal scratches of a depth of 0.3 cm) (Figure 1B), and (iv) fibroblast/astrocyte coculture with the scratch for 3 days followed by siRNA treatment for 4 days.

RNAi

The EphB2-specific siRNAs were synthesized by Nantong Biomics Biotechnologies Co., Ltd. (Nantong, China). We evaluated three candidate siRNAs—siRNA1, siRNA2, and siRNA3—for specificity and effectiveness (Table 1). The most specific and effective siRNA was selected using real-time polymerase chain reaction. For siRNA treatment, when the cells grew to 50% confluence, 30 nM siRNA and SuperFectin™ II reagent (Pufei Co., Ltd., Shanghai, China) were added, respectively, to the corresponding groups. After 48 hours, mRNA was extracted from the cells in the different groups, and proteins were extracted 4 days later.

Table 1 | Synthesized siRNA sequences for EphB2 silencing

siRNA name	Sequence (5'–3')	Decoration
EphB2-siRNA1	Sense: GAG AUC UUU GUA UCC AUC A-dTdT	FAM
	Antisense: UGA UGG CUA CAA AGA UCU C-dTdT	FAM
EphB2-siRNA2	Sense: AGA AGG AGC UCA GUG AGU A-dTdT	FAM
	Antisense: UAC UCA CUG AGC UCC UUC U-dTdT	FAM
EphB2-siRNA3	Sense: ACA AGG AGA GCU UUA CCA A-dTdT	FAM
	Antisense: UUG GUA AAG CUC UCC UUG U-dTdT	FAM

dTdT: Deoxythymidine dinucleotide; FAM: 5'-fluorescein phosphoramidite; siRNA: small interfering RNA.

Observation of the effect of silencing EphB2 on axon growth in the microfluidic platform

To evaluate the impact of the microenvironment on axon growth, we designed a microfluidic platform that was constructed by Suzhou Wenhao Chip Technology Co., Ltd. (Suzhou, China). The platform had three chambers, the middle of which was 15-mm long, 10-mm wide and 5-mm high, and represented the scar chamber. The two other chambers were 15-mm long, 5-mm wide and 5-mm high, and were used as soma chambers. Approximately 200 microchannels were present, each 250- μ m long, 15- μ m wide and 5- μ m high, between the adjacent chambers to guide axon growth.

Before use, the chambers were washed and UV-irradiated. In addition to the four groups mentioned above, another two groups were used as controls. In the scar chamber, DMEM/F12 containing 10% FBS was used as the negative control, and 5 μ g/mL CSPGs (Merck-Millipore, Schwalbach, Germany) were added to the positive control. Five thousand VSC4.1 motoneurons were cultured with 200 μ L DMEM/F12 containing 5% FBS in the two soma chambers. At the same time, 5 μ g/mL CSPGs or DMEM/F12 containing 10% FBS or a fibroblast/astrocyte coculture was added to the scar chamber. The following day, the medium in the soma chambers was replaced with DMEM/F12 containing 0.5% FBS for differentiation, and the fibroblast/astrocyte coculture in the scar chamber was scratched. Three days later, the designated groups were treated with 30 nM siRNA for another 4 days. Finally, axons were observed on an IX71 microscope (Olympus Corp., Hachioji, Tokyo, Japan), and their lengths were measured using DP2-BSW (Olympus Corp.).

Immunocytochemistry

The samples were fixed in 4% paraformaldehyde, rinsed with phosphate-buffered saline (Beyotime Biotechnology, Nantong, China), blocked with 0.3% Triton-X 100 and 3% bovine serum albumin, and incubated at 4°C overnight with primary antibodies—mouse anti-gial fibrillary acidic protein (1:400; Abcam, Cambridge, UK, Cat# ab21837) and rabbit anti-fibronectin (1:200; Abcam, Cat# ab23751). After rinsing with phosphate-buffered saline, the samples were incubated with secondary antibodies—Alexa Fluor 488-labeled donkey anti-mouse IgG (1:1,000; Thermo Fisher, Cat# A21202) or Alexa Fluor 568-labeled donkey anti-rabbit IgG (1:1,000; Thermo Fisher, Cat# A10042) at room temperature for 2 hours in the dark. Finally, the specimens were sealed with 4',6-diamidino-2-phenylindole-containing sealant (Vector Laboratories, Burlingame, CA, USA) and observed under a laser-scanning confocal microscope (SP7, Leica, Wetzlar, Germany).

Real-time polymerase chain reaction

During formation of the glial/fibrotic scar, EphB2 and ephrin-B2 mRNAs were detected at different time points (4 hours, and 2, 4, 7 and 14 days) after scratching. The effect of EphB2 RNAi was also assessed. The primers, synthesized by Invitrogen Corp. (Carlsbad, CA, USA), are listed in **Table 2**. Total RNA was extracted using the QIAcube Automated RNA Extractor (QIAGEN, Chatsworth, CA, USA). Glyceraldehyde-3-phosphate dehydrogenase was used as an internal reference control, and the non-templated wells were used as negative control. The $2^{-\Delta\Delta Ct}$ relative quantitative analysis method was used to evaluate expression levels.

Western blot assay

The cells were lysed in 1 \times radioimmunoprecipitation assay buffer (Beyotime Biotechnology), and the protein concentrations were measured. For neurocan, NG2 and collagen I, 6% sodium dodecyl sulfate polyacrylamide gels were used for electrophoresis, and the proteins were transferred onto a polyvinylidene fluoride membrane at 150 mA for 16 hours. For other proteins, 8% gels were used, and transfer was performed at 75 V for 1 hour. After blocking for 2

Table 2 | Primer sequences for polymerase chain reaction

Primer	Sequence (5'–3')	Product size (bp)
GAPDH	Sense: GCA AGT TCA ACG GCA CAG	141
	Antisense: CGC CAG TAG ACT CCA CGA C	
EphB2	Sense: CAC CGA CCA GAG TCC CTT	215
	Antisense: ATG GCT GTG GCG TTG TAC	
ephrin-B2	Sense: GTT ATC ATA CCG CTA AGG A	127
	Antisense: TAG TAA ATG TTG GCA GGA C	

GAPDH: Glyceraldehyde-3-phosphate dehydrogenase.

hours at room temperature with 5% skim milk in Tris-buffered saline/0.1% Tween 20, the membranes were incubated with the following primary antibodies overnight at 4°C: mouse anti-neurocan (1:1000; Abcam, Cat# ab31979), mouse anti-NG2 (1:1000; Abcam, Cat# ab50009), rabbit anti-collagen I (1:1000; Abcam, Cat# ab260043), rabbit anti-EphB2 (1:1000; Cell Signaling Technology, Cat# 83029), rabbit anti-ephrin-B2 (1:1000; Abcam, Cat# ab150411), mouse anti-glyceraldehyde-3-phosphate dehydrogenase (1:5000; Sigma-Aldrich, St. Louis, MO, USA, Cat# MAB374) and mouse anti- β -actin (1:5000; Sigma-Aldrich, Cat# A5441). The following day, the membranes were incubated for 2 hours at room temperature with secondary antibody—horseradish peroxidase-conjugated anti-mouse IgG (1:5000; Sigma-Aldrich, Cat# A3682) or horseradish peroxidase-conjugated anti-rabbit IgG (1:5000; Sigma-Aldrich, Cat# A0545). The immunoreactive bands were visualized using an enhanced chemiluminescence kit (Bio-Rad Laboratories Inc., Hercules, CA, USA) and analyzed using Image Lab (Bio-Rad Laboratories).

Statistical analysis

Data are presented as the mean \pm standard deviation (SD). GraphPad Prism 6.0 (GraphPad Software, San Diego, CA, USA) was used for data analyses and image generation. Data were first subjected to analysis of homogeneity of variance. Then the data from the real-time polymerase chain reaction, western blotting and axon length measurements were analyzed using one-way analysis of variance. For statistically significant results, multiple comparisons between groups were made with least significant difference test. $P < 0.05$ was considered statistically significant.

Results

Morphological changes in fibroblasts and astrocytes after scratch treatment

Fibroblasts and astrocytes were seeded into two adjacent chambers (**Figure 1B**). After 1 hour, all of the cells were attached to the slide, and the upper shelf was removed. The cells on the slide were then cultured in 100-mm dishes (**Figure 1C**). Three days later, different treatments were performed according to the experimental design. The immunostaining showed that fibroblasts and astrocytes expressed fibronectin and glial fibrillary acidic protein, respectively. Without any treatment, the two types of cells remained separated on each side and rarely intersected at the interface (**Figure 1D1–D3, d3** and **Additional Figure 1A**). In comparison, after the scratch treatment, the two types of cells began to migrate, especially fibroblasts, which infiltrated the astrocytic side along the scratched region (**Additional Figure 1B** and **C**). Seven days after the scratch treatment, the two cell types were arranged close together, over which the astrocytes with their elongated processes contacted the fibroblasts, in a manner resembling a fence (**Figure 1E1–E3, e3**).

Changes in EphB2 and ephrin-B2 expression after scratch treatment

Changes in *EphB2* and *ephrin-B2* expression were assessed at different time points after scratch treatment. The real-time polymerase chain reaction data showed that *EphB2* expression

after scratch treatment increased with time ($P < 0.05$), except at 4 hours, when there was no significant change compared with the untreated group ($P > 0.05$; **Figure 2A**). Expression of *ephrin-B2* after scratch treatment was significantly upregulated from day 2 compared with the untreated group ($P < 0.05$); however, during our observation period, there was no significant change at 4, 7 or 14 days ($P > 0.05$; **Figure 2B**).

Changes in the protein expression levels of EphB2 and ephrin-B2 at different time points after scratch treatment were also examined. The western blot results showed that compared with the untreated group, EphB2 protein increased from day 4 after scratch treatment ($P < 0.05$), but with no significant change between 7 and 14 days ($P > 0.05$; **Figure 2C** and **2D**). The upregulation of ephrin-B2 protein began on day 2 ($P < 0.05$), but there were no significant changes between 7 and 14 days ($P > 0.05$; **Figure 2C** and **2E**).

Effects of siRNAs against EphB2 and ephrin-B2 on changes induced by scratch

Real-time polymerase chain reaction was used to screen the efficiency of siRNA-1, siRNA-2 and siRNA-3 at 48 hours after RNAi treatment. Compared with the control, the relative expression of *EphB2* significantly decreased after RNAi treatment. Among the siRNAs, siRNA2 had the strongest effect ($P < 0.05$ or $P < 0.01$; **Figure 3A**), and was thus used for subsequent experiments.

When both scratch and siRNA treatments were used on the fibroblasts and astrocytes, the mRNA levels of *EphB2* were considerably lower compared with scratch alone (**Figure 3B**); however, this was not observed for ephrin-B2, indicating that siRNA against EphB2 did not affect the expression of ephrin-B2 (**Figure 3C**).

Immunostaining showed that when only the scratch treatment was applied to the fibroblasts and astrocytes, the two types of cells became densely arranged. Astrocytes extended elongated processes that crossed with fibroblasts (**Figure 3D1–D3, d3**). However, when the fibroblasts and astrocytes were scratch-treated for 3 days and then with siRNA-2 targeting EphB2 for 4 days, the cells were loosely arranged and dispersed, with no crossings between the two types of cells. Furthermore, there were no compact bands of cells (**Figure 3E1–E3, e3**).

Effects of RNAi on axon growth in microfluidic platforms

The three-chambered microfluidic platforms were used to assess the effect of siRNA targeting EphB2 on axon growth into the glial/fibrotic scar (**Figure 4A**). In this device, VSC4.1 motoneurons extended their axons from the soma chambers to the central scar chamber where the various treatment groups were cultured (**Figure 4B**). **Figure 4C–H** shows the results. We observed that motor axons grew for 4–5 days and entered the scar chamber along the microchannels without scratch treatment (**Figure 4E** and **e**). VSC4.1 motoneuron axons entered the scar chamber with the fibroblast/astrocyte coculture given scratch treatment or with the addition of CSPGs as a positive control. Notably, when the axons neared the scar chamber, their growth appeared to be hampered, and some had even withdrawn, as shown by the presence of retraction bulbs at the terminals (**Figure 4D, G** and **g**). When the fibroblast/astrocyte coculture was treated with siRNA alone, some of the motor axons were able to extend somewhat further into the scar chamber (**Figure 4F**). Compared with the scratch treatment alone, the coculture given both the scratch and siRNA treatments showed markedly increased axon growth, and small bulb structures at the axon terminals were not evident (**Figure 4H** and **h**).

Statistical analysis of axon growth length suggested that scratch treatment of the fibroblast/astrocyte coculture significantly reduced motor axon growth compared with

no treatment ($P < 0.05$). In contrast, when siRNA was used to suppress the upregulation of EphB2 in the scratch-treated fibroblast/astrocyte coculture, the analysis revealed significantly greater axon growth ($P < 0.05$). Compared with the blank control in which the scar chamber was filled with DMEM/F12 containing 10% FBS, the length of motor axons was reduced in the other three groups, i.e., the positive control group (in which CSPGs were added to the scar chamber), the fibroblast/astrocyte coculture that was scratch-treated, and the fibroblast/astrocyte coculture that was treated with both scratch and siRNA ($P < 0.05$). Compared with the positive control, the motor axons were longer when the scar chamber was cultured with the fibroblast/astrocyte coculture, given siRNA treatment only, or given both scratch and siRNA treatments ($P < 0.05$; **Figure 4I**).

Effects of RNAi on ECM components in fibroblast/astrocyte cocultures

Western blot analysis showed that scratch treatment increased the protein levels of neurocan, NG2 and collagen I in the fibroblast/astrocyte coculture more than in the no-treatment group ($P < 0.05$). After adding siRNA targeting EphB2, there was a statistically significant decrease in neurocan, NG2 and collagen I proteins compared with cocultures given scratch treatment alone ($P < 0.05$; **Figure 5A–E**).

Discussion

In the present study, we developed an *in vitro* glial/fibrotic scar model by coculturing fibroblasts and astrocytes with scratch treatment in an improved slide system. A Chinese invention patent (Patent No. ZL 2015 1 0292819.4) has been granted to this glial/fibrotic scar model. When the microfluidic chip designed by our team was used to test the effect of the glial/fibrotic scar on neuronal axon growth, we observed that the scar had a negative regulatory effect on growth. Notably, after knocking down EphB2, which is considered to have a key role in the initial stages of glial/fibrotic scar formation, not only were the two types of cells loosely arranged, but the inhibitory effect on axon growth was partially alleviated.

Following SCI, astrocytes are activated and produce ECMs that contribute to glial scar formation (Chen et al., 2016). At the same time, the lesion is invaded by fibroblasts, not only derived from proliferating meningeal cells, but also from perivascular cells (Göritz et al., 2011; Soderblom et al., 2013; Dias et al., 2018), which also secrete ECM components to form fibrous scars. Migration, arrangement and aggregation of the two types of cells result in the formation of glial/fibrotic scars. Although other cell types may also participate in this process (Chen et al., 2016; Funk et al., 2016), fibroblasts and astrocytes are undoubtedly the two most important cell components of glial/fibrotic scars. Consequently, we established a model of glial/fibrotic scars *in vitro* using fibroblasts and astrocytes. In previous studies, the model was produced by separately culturing fibroblasts and astrocytes to observe changes at the boundary between these cells (Shearer et al., 2003), or by allowing them to grow together with/without transforming growth factor- β 1 (Wanner et al., 2008; Kimura-Kuroda et al., 2010). In the present study, given that traumatic SCI is commonly seen after accidents, such as traffic accidents, natural disasters and violent sports, we chose mechanical scratch damage to mimic the injury. Interestingly, in the experimental groups, the fibroblasts and astrocytes migrated, rearranged, aggregated, intertwined, and formed compact cell bands. Moreover, the astrocytes exhibited an activated state during which the processes became longer and accumulated glial fibrillary acidic protein, consistent with previous studies (Pekny and Nilsson, 2005; Sofroniew, 2005; Wanner et al., 2008).

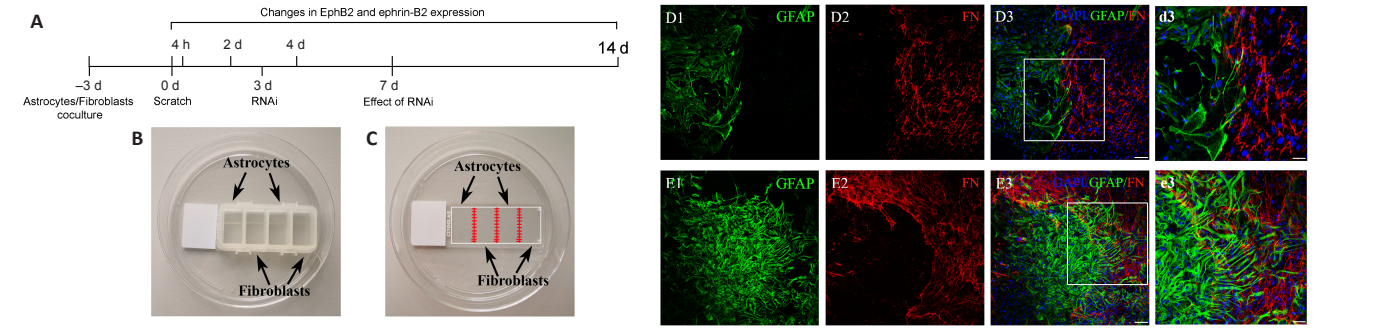


Figure 1 | Fibroblast/astrocyte coculture with scratch treatment.

(A) The experimental timeline. (B) Photograph of an improved slide system which is made up of a slide and a shelf removed from the Lab-Tek chamber slide. Purified fibroblasts and astrocytes were seeded in two adjacent chambers. (C) Photograph showing the scratch treatment (red lines) at the interface. After cell attachment, the shelf is removed. Three days later, the scratch treatment was performed as shown in the schematic diagram. (D1–3, d3) Immunofluorescence staining of fibroblast/astrocyte cocultured for 7 days without scratch treatment. Purified astrocytes and fibroblasts, identified by labeling for GFAP (green, Alexa Fluor 488) and FN (red, Alexa Fluor 568), respectively, grew on each side separately, and no obvious aggregation was observed. (E1–3, e3) Immunofluorescence staining of fibroblast/astrocyte cocultures following scratch treatment. The two types of cells were associated tightly, among which astrocytes with their elongated processes crossed over the fibroblasts. Dense cell bands were formed. d3 and e3 are enlarged images of the area in the rectangles in D3 and E3. Scale bars: 100 μ m in D1–3 and E1–3; 50 μ m in d3 and e3. FN: Fibronectin; GFAP: glial fibrillary acidic protein.

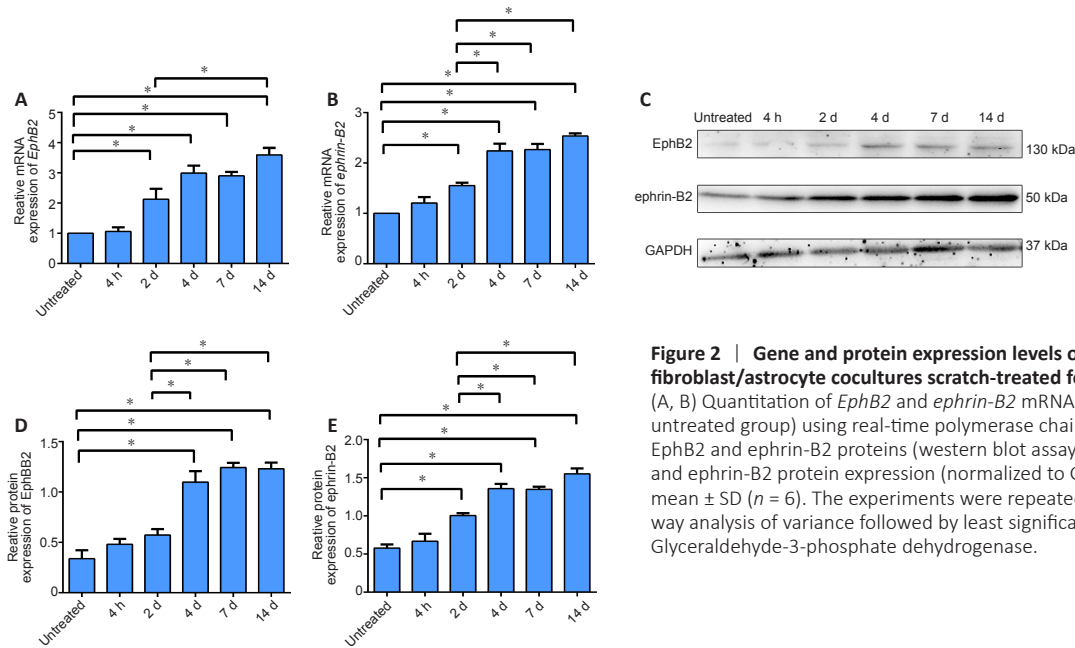


Figure 2 | Gene and protein expression levels of EphB2 and ephrin-B2 in fibroblast/astrocyte cocultures scratch-treated for different time points.

(A, B) Quantitation of *EphB2* and *ephrin-B2* mRNA expression (normalized to the untreated group) using real-time polymerase chain reaction. (C) Immunoblots of *EphB2* and *ephrin-B2* proteins (western blot assay). (D, E) Quantitation of *EphB2* and *ephrin-B2* protein expression (normalized to GAPDH). Data are expressed as mean \pm SD ($n = 6$). The experiments were repeated three times. * $P < 0.05$ (one-way analysis of variance followed by least significant difference test). GAPDH: Glyceraldehyde-3-phosphate dehydrogenase.

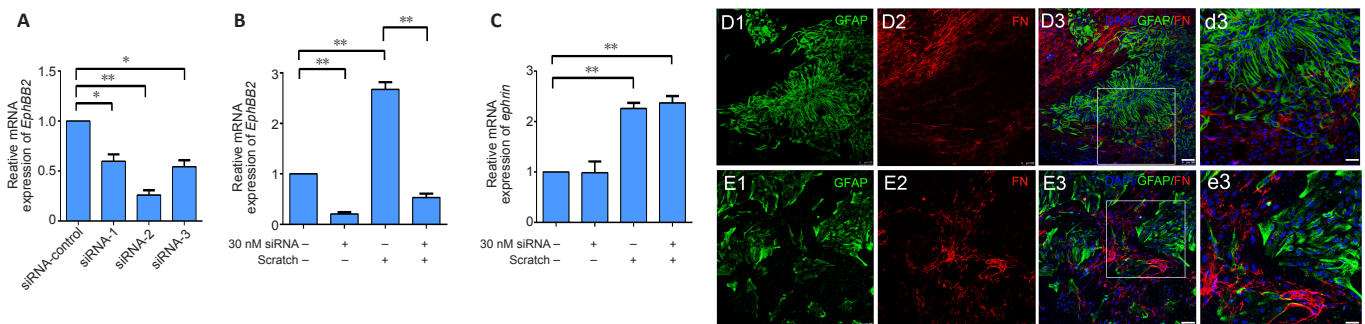


Figure 3 | siRNA screening and its effect on fibroblast/astrocyte cocultures given different treatments.

(A) Gene expression of *EphB2* in fibroblasts treated with different siRNA sequences. siRNA-control is a non-coding control; siRNA-1, siRNA-2 and siRNA-3 represent different coding sequences. (B, C) Gene expression levels of *EphB2* and *ephrin-B2* in fibroblast/astrocyte cocultures given scratch and/or siRNA treatment. Data are expressed as mean \pm SD. The experiments were repeated six times. * $P < 0.05$, ** $P < 0.01$. (D1–3, d3) Immunofluorescence staining for FN for fibroblasts (red, Alexa Fluor 568) and GFAP for astrocytes (green, Alexa Fluor 488) in cocultures following scratch treatment for 7 days. (E1–E3, e3) Immunofluorescence staining of fibroblast/astrocyte cocultures following scratch treatment for 3 days and then siRNA targeting *EphB2* for 4 days. The cells were arranged uniformly and dispersed compared with without RNAi. d3 and e3 are the enlarged images of the areas in rectangles in D3 and E3. Scale bars: 100 μ m in D1–3 and E1–3; 50 μ m in d3 and e3. FN: Fibronectin; GFAP: glial fibrillary acidic protein; RNAi: RNA interference; siRNA: small interfering RNA.

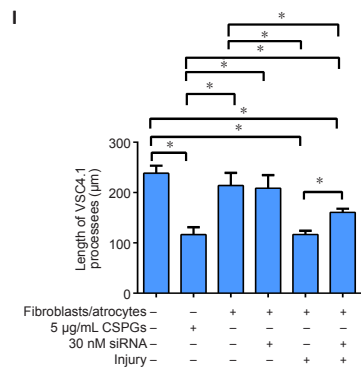
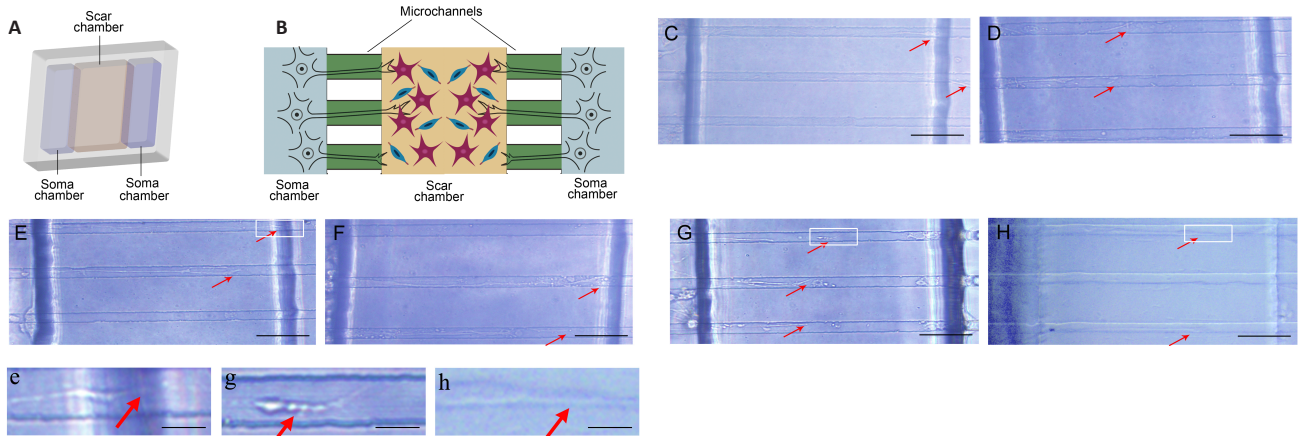


Figure 4 | VSC4.1 motoneuron axon growth to the scar chamber in microfluidic platforms.

(A) Computer-aided design picture of a microfluidic platform. (B) Structural diagram of a microfluidic platform. The fibroblast/astrocyte coculture was in the middle axon/scar chamber, while VSC4.1 motoneurons were cultured in the two soma chambers. Between adjacent chambers, microchannels were present, which could guide axonal growth from the soma chambers to axon/scar chambers. (C–H) Photomicrographs showing axon growth in each group in the microchannels. The axons of VSC4.1 motoneurons could enter the scar chamber along the microchannels in the blank control (C). In the positive control in which CSPGs were added, axon growth was reduced, and bulb structures appeared at the axon terminals (D) and in the group in which the fibroblast/astrocyte coculture was scratched (G, g). The axons of VSC4.1 motoneurons were long in the microchannels when the fibroblast/astrocyte coculture in the scar chamber was given no treatment (E, e) or with siRNA treatment (F). Then, 4 or 5 days later, when the fibroblast/astrocyte coculture was treated with scratch and siRNA, VSC4.1 motoneuron axons were longer compared with scratch alone, and there were smaller bulbs at the axon terminals (H, h). e, g and h are enlarged images of the areas in the rectangles in E, G and H. Arrows show axons or bulbs of axons. Scale bars: 50 µm in C–H; 10 µm in e, g and h. (I) Bar graph showing the difference in axon length after 7 days of culture in the microfluidic platform. Data are expressed as mean ± SD ($n = 8$). The experiments were repeated three times. * $P < 0.05$ (one-way analysis of variance followed by least significant difference test). CSPG: chondroitin sulfate proteoglycan; siRNA: small interfering RNA.

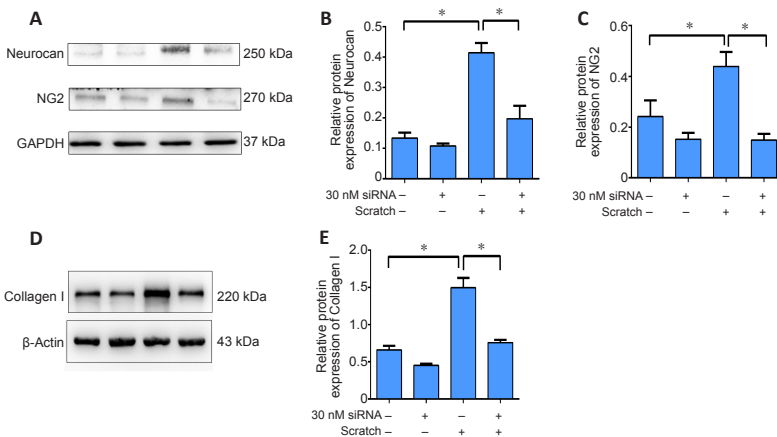


Figure 5 | Western blot showing expression of neurocan, NG2 and collagen I in fibroblast/astrocyte cocultures given treatment with scratch and/or siRNA targeting EphB2.

(A) Representative blots for neurocan and NG2 proteins. (B, C) Bar graph showing quantitation of neurocan and NG2 protein expression (normalized to GAPDH). (D) Representative blots for collagen I protein. From left to right, the sequence of the blot is consistent with that of the bar diagram below. (E) Bar graph showing quantitation of collagen I protein (normalized to β-actin). Data are expressed as mean ± SD ($n = 6$). The experiments were repeated three times. * $P < 0.05$ (one-way analysis of variance followed by least significant difference test). GAPDH: Glyceraldehyde-3-phosphate dehydrogenase; siRNA: small interfering RNA.

Aside from their important roles in axon guidance in CNS development (Shen and Cowan, 2010), the involvement of Ephs/ephrins in complex pathological process and in the structural and functional reorganization of the damaged CNS has become fairly well known (Cramer and Miko, 2016; Yang et al., 2018). For example, the EphA4 receptor is an inhibitor of neural regeneration, and accumulates in both damaged corticospinal axons and reactive astrocytes after SCI (Du et al., 2007; Fabes et al., 2007). In dorsal hemisection injury, compared with wild-type mice, corticospinal and raphespinal growth is increased in the caudal spinal cord in ephrin-B3^{-/-} mice 6 weeks after injury, and exercise capacity is improved in the open field by kinematic analysis (Duffy et al., 2012). Bundesen et al. (2003) found that invading meningeal fibroblasts upregulate EphB2 and astrocytes upregulate ephrin-B2 and form a characteristic scar around the lesion site.

In the experimental groups, EphB2 and ephrin-B2 mRNAs and proteins were upregulated. The upregulation of EphB2 and ephrin-B2 indicates that they play a role in the formation of glial/fibrotic scars from the onset of scar formation, and thus both EphB2 and ephrin-B2 are potential targets for inhibiting scar formation. In fact, we found that RNAi-mediated ephrin-B2 silencing attenuates glial/fibrotic scar formation (Li et al., 2017). However, if RNAi technology is applied *in vivo* in future studies, we may use the lowest virus titer and the least number of cells to minimize the negative effects. In the CNS, meningeal fibroblasts are far fewer than astrocytes (Kania and Klein, 2016). Moreover, the view that astrocytic scar formation favors axonal regeneration in the CNS (Anderson et al., 2016) has attracted attention towards fibroblasts (Hara et al., 2017; Dias et al., 2018). Additionally, we found that siRNA targeting EphB2 had a greater inhibitory effect on glial/fibrotic scar

Research Article

formation (**Additional Figure 2**). Therefore, we used RNAi to inhibit the upregulation of EphB2 expression. Our data show that silencing EphB2 reduces cell aggregation, resulting in an irregular and loose arrangement of fibroblasts and astrocytes.

To observe the effect of EphB2 silencing on axon growth, we used a special microfluidic platform with three chambers. The chamber for glial/fibrotic scar formation was in the middle and two soma chambers were on either side. Between adjacent chambers, there were approximately 200 microchannels for guiding axon growth. There are various descending fiber tracts in the spinal cord, which project from different brain regions and have different morphologies. We selected VSC4.1 motoneurons, which are commonly used in studies of the CNS, to observe the impact of various microenvironments on axon growth. Because the microchannels are 5- μm high, 15- μm wide and 250- μm long, somata of VSC4.1 motoneurons were prevented from leaving the side chambers, and the axons and dendrites could be more clearly observed. We observed that the axons of VCS4.1 motoneurons could enter the middle scar chamber through the microchannels. When the fibroblasts and astrocytes were cocultured inside the scar chamber, not all axons could enter into the middle chamber. When glial/fibrotic scars formed after scratch treatment, axon growth was considerably inhibited. The same result was observed when CSPGs alone were added to the scar chamber. When the fibroblast/astrocyte coculture received both the scratch and siRNA treatments, axon growth markedly improved, suggesting that downregulating EphB2 inhibits formation of the glial/fibrotic scar, and is therefore beneficial to axon growth. We speculate that inhibitory factors derived from the scar chamber were present in the microchannels, which might have resulted in axon retraction in the scratch-treated coculture. This is consistent with the results of Hur et al. (2011), who found that some axons turn back and re-enter the microchannels to avoid contact with CSPGs. CSPGs include neurocan, versican, brevican, NG2 and phosphacan (Siebert et al., 2014). After SCI, they show different patterns of change in expression and are derived from different cell types. Neurocan, a unique CSPG, is synthesized by astrocytes and is the first to appear in the center of the lesion, increases within days, and peaks at 2 weeks (Jones et al., 2003). NG2, also known as CSPG4, is also upregulated, and its expression peaks 1 week after SCI (Andrews et al., 2012). NG2 is expressed in cultured meningeal fibroblasts (Shearer et al., 2003). After the culture is treated with anti-NG2 antibodies, neurite outgrowth is increased (Minor et al., 2008). Fibroblasts also synthesize collagen I, which is implicated in the induction of astrogliosis and the deposition of ECM molecules, and is a major mechanical barrier for axon growth (Nathan and Li, 2017). In the present study, we observed that neurocan, NG2 and collagen I proteins were markedly increased in the scratch treatment group. After reducing EphB2 using RNAi, these proteins were downregulated, indicating that EphB2-specific RNAi not only reduces the expression of EphB2 mRNA, but also decreases the secretion of ECMs.

In conclusion, downregulation of EphB2 by RNAi may alleviate the formation of the glial/fibrotic scar, which is induced by two injury-related factors—scratch treatment and meningeal fibroblast infiltration. EphB2 downregulation also reduces the production of ECM components that are inhospitable for axonal regeneration, thereby improving the microenvironment and allowing axons to grow longer. These findings are based on *in vitro* experiments, and therefore, validation with *in vivo* experiments is warranted. Moreover, the binding of Eph family and its ligand is not in the one-to-one mode, and there may be other receptors or ligands involved, which needs further exploration.

Acknowledgments: VSC4.1 motoneurons were provided as a gift by Dr. Weidong Le at Baylor College of Medicine (Houston, TX, USA).

Author contributions: Study and microfluidic platform design: JW, YL. All authors participated experiments, analyzed data, contributed to writing of the manuscript, and approved the final version of manuscript for publication.

Conflicts of interest: The authors declare that there are no conflicts of interest associated with this manuscript.

Financial support: This work was supported by the Priority Academic Program Development of Jiangsu Higher Education Institutes of China (PAPD); the Science and Technology Plan Project of Nantong of China, No. JC2020026 (to JW); the National Science Research of Jiangsu Higher Education Institutions of China, No. 19KJB310012 (to RYY). The funding sources had no role in study conception and design, data analysis or interpretation, paper writing or deciding to submit this paper for publication.

Institutional review board statement: This study was approved by the the Laboratory Animal Ethics Committee of Jiangsu Province, China (approval No. 2019-0506-002) on May 6, 2019.

Copyright license agreement: The Copyright License Agreement has been signed by all authors before publication.

Data sharing statement: Datasets analyzed during the current study are available from the corresponding author on reasonable request.

Plagiarism check: Checked twice by iThenticate.

Peer review: Externally peer reviewed.

Open access statement: This is an open access journal, and articles are distributed under the terms of the Creative Commons Attribution-NonCommercial-ShareAlike 4.0 License, which allows others to remix, tweak, and build upon the work non-commercially, as long as appropriate credit is given and the new creations are licensed under the identical terms.

Open peer reviewer: Susan Goulding, University College Cork, Ireland.

Additional files:

Additional file 1: Open peer review report 1.

Additional Figure 1: Fibroblast/astrocyte coculture without/with scratch treatment.

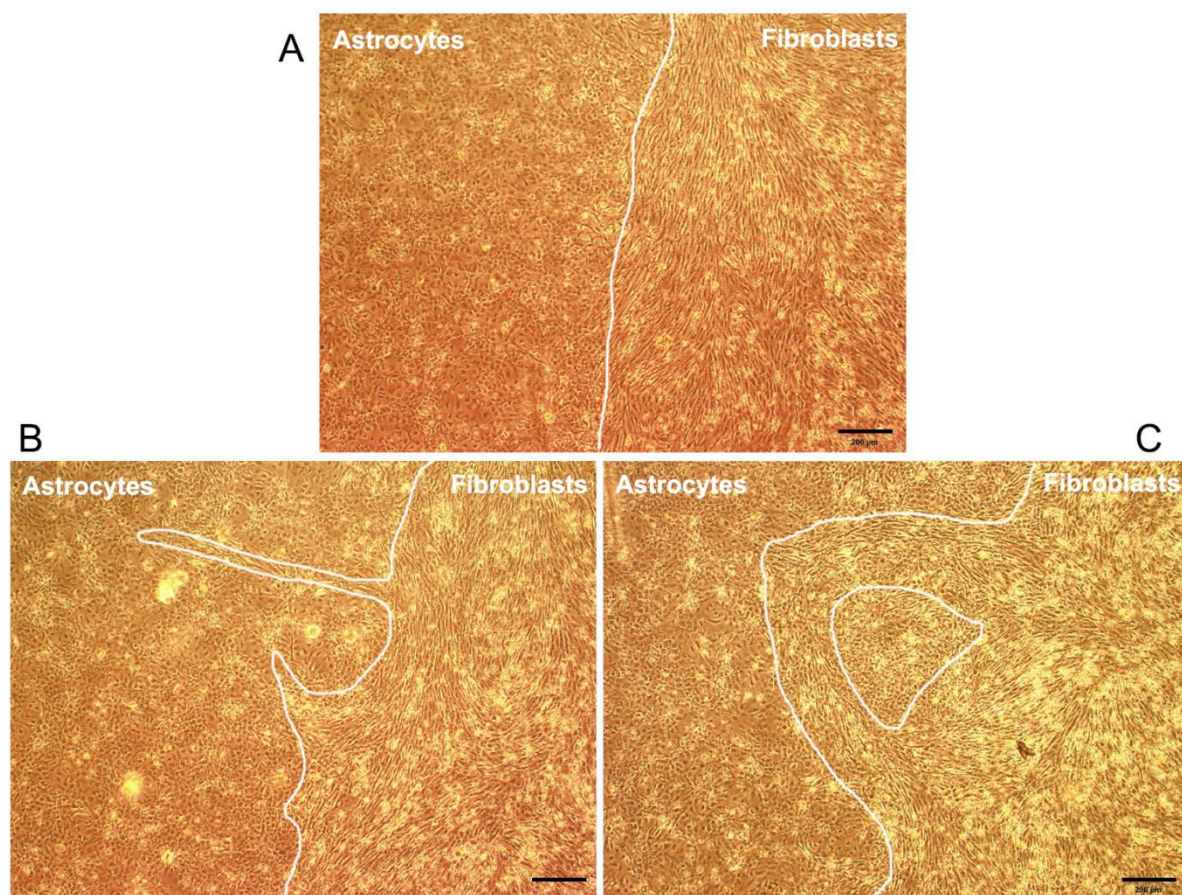
Additional Figure 2: Co-culture of astrocytes and fibroblasts with different treatments.

References

- Abnet K, Fawcett JW, Dunnett SB (1991) Interactions between meningeal cells and astrocytes in vivo and in vitro. *Brain Res Dev Brain Res* 59:187-196.
- Anderson MA, Burda JE, Ren Y, Ao Y, O'Shea TM, Kawaguchi R, Coppola G, Khakh BS, Deming TJ, Sofroniew MV (2016) Astrocyte scar formation aids central nervous system axon regeneration. *Nature* 532:195-200.
- Andrews EM, Richards RJ, Yin FQ, Viapiano MS, Jakeman LB (2012) Alterations in chondroitin sulfate proteoglycan expression occur both at and far from the site of spinal contusion injury. *Exp Neurol* 235:174-187.
- Bundesen LQ, Scheel TA, Bregman BS, Kromer LF (2003) Ephrin-B2 and EphB2 regulation of astrocyte-meningeal fibroblast interactions in response to spinal cord lesions in adult rats. *J Neurosci* 23:7789-7800.
- Chakrabarti M, Banik NL, Ray SK (2014) MiR-7-1 potentiated estrogen receptor agonists for functional neuroprotection in VSC4.1 motoneurons. *Neuroscience* 256:322-333.
- Chen CH, Sung CS, Huang SY, Feng CW, Hung HC, Yang SN, Chen NF, Tai MH, Wen ZH, Chen WF (2016) The role of the PI3K/Akt/mTOR pathway in glial scar formation following spinal cord injury. *Exp Neurol* 278:27-41.
- Choi EH, Gattas S, Brown NJ, Hong JD, Limbo JN, Chan AY, Oh MY (2021) Epidural electrical stimulation for spinal cord injury. *Neural Regen Res* 16:2367-2375.
- Cramer KS, Miko IJ (2016) Eph-ephrin signaling in nervous system development. *F1000Res* 5:F1000 Faculty Rev-413.
- Dias DO, Kim H, Holl D, Werne Solnestam B, Lundeberg J, Carlén M, Göritz C, Frisén J (2018) Reducing pericyte-derived scarring promotes recovery after spinal cord injury. *Cell* 173:153-165.e22.
- Donia A, Bokhari H (2021) RNA interference as a promising treatment against SARS-CoV-2. *Int Microbiol* 24:123-124.
- Du J, Fu C, Sretavan DW (2007) Eph/ephrin signaling as a potential therapeutic target after central nervous system injury. *Curr Pharm Des* 13:2507-2518.
- Duffy P, Wang X, Siegel CS, Tu N, Henkemeyer M, Cafferty WB, Strittmatter SM (2012) Myelin-derived ephrinB3 restricts axonal regeneration and recovery after adult CNS injury. *Proc Natl Acad Sci U S A* 109:5063-5068.

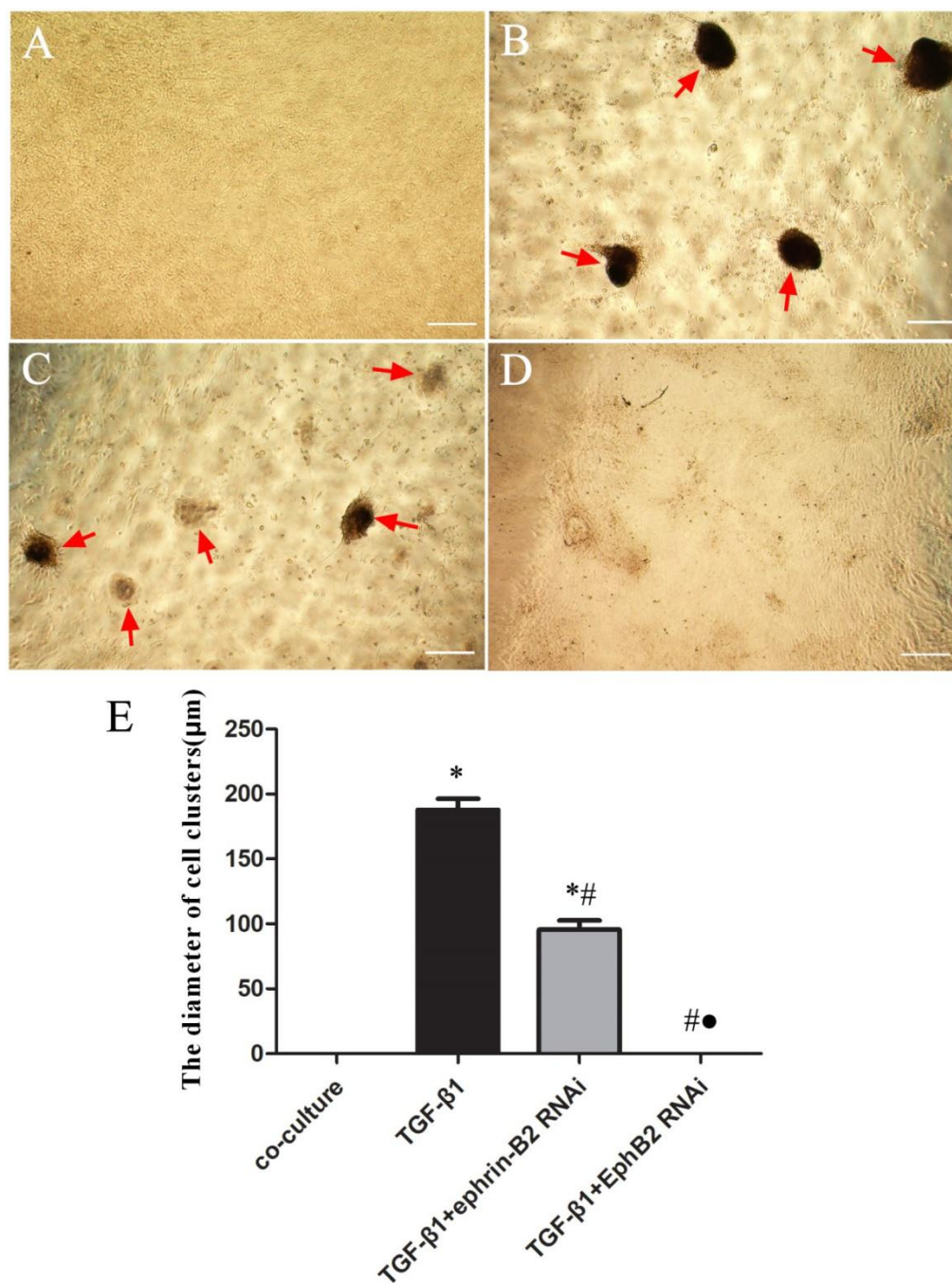
- Dun XP, Parkinson DB (2020) Classic axon guidance molecules control correct nerve bridge tissue formation and precise axon regeneration. *Neural Regen Res* 15:6-9.
- Fabes J, Anderson P, Brennan C, Bolsover S (2007) Regeneration-enhancing effects of EphA4 blocking peptide following corticospinal tract injury in adult rat spinal cord. *Eur J Neurosci* 26:2496-2505.
- Ferguson R, Subramanian V (2016) PA6 stromal cell co-culture enhances SH-SY5Y and VSC4.1 neuroblastoma differentiation to mature phenotypes. *PLoS One* 11:e0159051.
- Funk LH, Hackett AR, Bunge MB, Lee JK (2016) Tumor necrosis factor superfamily member APRIL contributes to fibrotic scar formation after spinal cord injury. *J Neuroinflammation* 13:87.
- Goldshmit Y, Mclenachan S, Turnley A (2006) Roles of Eph receptors and ephrins in the normal and damaged adult CNS. *Brain Res Rev* 52:327-345.
- Göritz C, Dias DO, Tomilin N, Barbacid M, Shupliakov O, Frisen J (2011) A pericyte origin of spinal cord scar tissue. *Science* 333:238-242.
- Hara M, Kobayakawa K, Ohkawa Y, Kumamaru H, Yokota K, Saito T, Kijima K, Yoshizaki S, Harimaya K, Nakashima Y, Okada S (2017) Interaction of reactive astrocytes with type I collagen induces astrocytic scar formation through the integrin-N-cadherin pathway after spinal cord injury. *Nat Med* 23:818-828.
- Hur EM, Yang IH, Kim DH, Byun J, Sajjilafu, Xu WL, Nicovich PR, Cheong R, Levchenko A, Thakor N, Zhou FQ (2011) Engineering neuronal growth cones to promote axon regeneration over inhibitory molecules. *Proc Natl Acad Sci U S A* 108:5057-5062.
- Hussein RK, Mencio CP, Katagiri Y, Brake AM, Geller HM (2020) Role of chondroitin sulfation following spinal cord injury. *Front Cell Neurosci* 14:2008.
- Jones LL, Margolis RU, Tuszynski MH (2003) The chondroitin sulfate proteoglycans neurocan, brevican, phosphacan, and versican are differentially regulated following spinal cord injury. *Exp Neurol* 182:399-411.
- Kania A, Klein R (2016) Mechanisms of ephrin-Eph signalling in development, physiology and disease. *Nat Rev Mol Cell Biol* 17:240-256.
- Karimi-Abdolrezaee S, Eftekharpour E, Wang J, Schut D, Fehlings MG (2010) Synergistic effects of transplanted adult neural stem/progenitor cells, chondroitinase, and growth factors promote functional repair and plasticity of the chronically injured spinal cord. *J Neurosci* 30:1657-1676.
- Kimura-Kuroda J, Teng X, Komuta Y, Yoshioka N, Sango K, Kawamura K, Raisman G, Kawano H (2010) An in vitro model of the inhibition of axon growth in the lesion scar formed after central nervous system injury. *Mol Cell Neurosci* 43:177-187.
- Li H, Wang C, He T, Zhao T, Chen YY, Shen YL, Zhang X, Wang LL (2019) Mitochondrial transfer from bone marrow mesenchymal stem cells to motor neurons in spinal cord injury rats via gap junction. *Theranostics* 9:2017-2035.
- Li Y, Chen Y, Tan L, Pan JY, Lin WW, Wu J, Hu W, Chen X, Wang XD (2017) RNAi-mediated ephrin-B2 silencing attenuates astroglial-fibrotic scar formation and improves spinal cord axon growth. *CNS Neurosci Ther* 23:779-789.
- Millet LJ, Gillette MU (2012) New perspectives on neuronal development via microfluidic environments. *Trends Neurosci* 35:752-761.
- Minor K, Tang X, Kahrilas G, Archibald SJ, Davies JE, Davies SJ (2008) Decorin promotes robust axon growth on inhibitory CSPGs and myelin via a direct effect on neurons. *Neurobiol Dis* 32:88-95.
- Nathan FM, Li S (2017) Environmental cues determine the fate of astrocytes after spinal cord injury. *Neural Regen Res* 12:1964-1970.
- Orr MB, Gensel JC (2018) Spinal cord injury scarring and inflammation: therapies targeting glial and inflammatory responses. *Neurotherapeutics* 15:541-553.
- Park JW, Kim HJ, Kang MW, Jeon NL (2013) Advances in microfluidics-based experimental methods for neuroscience research. *Lab Chip* 13:509-521.
- Pekny M, Nilsson M (2005) Astrocyte activation and reactive gliosis. *Glia* 50:427-434.
- Ren Z, Chen X, Yang J, Kress BT, Tong J, Liu H, Takano T, Zhao Y, Nedergaard M (2013) Improved axonal regeneration after spinal cord injury in mice with conditional deletion of ephrin B2 under the GFAP promoter. *Neuroscience* 241:89-99.
- Rosenzweig ES, Salegio EA, Liang JJ, Weber JL, Weinholtz CA, Brock JH, Moseanko R, Hawbecker S, Pender R, Cruzen CL, Iaci JF, Caggiano AO, Blight AR, Haenzi B, Huie JR, Havton LA, Nout-Lomas YS, Fawcett JW, Ferguson AR, Beattie MS, et al. (2019) Chondroitinase improves anatomical and functional outcomes after primate spinal cord injury. *Nat Neurosci* 22:1269-1275.
- Sami A, Selzer ME, Li S (2020) Advances in the signaling pathways downstream of glial-scar axon growth inhibitors. *Front Cell Neurosci* 14:174.
- Saw PE, Song EW (2020) siRNA therapeutics: a clinical reality. *Sci China Life Sci* 63:485-500.
- Schachtrup C, Ryu JK, Helmrick MJ, Vagena E, Galanakis DK, Degen JL, Margolis RU, Akassoglou K (2010) Fibrinogen triggers astrocyte scar formation by promoting the availability of active TGF-beta after vascular damage. *J Neurosci* 30:5843-5854.
- Shearer MC, Niclou SP, Brown D, Asher RA, Holtmaat AJ, Levine JM, Verhaagen J, Fawcett JW (2003) The astrocyte/meningeal cell interface is a barrier to neurite outgrowth which can be overcome by manipulation of inhibitory molecules or axonal signalling pathways. *Mol Cell Neurosci* 24:913-925.
- Shen K, Cowan CW (2010) Guidance molecules in synapse formation and plasticity. *Cold Spring Harb Perspect Biol* 2:a001842.
- Shomer NH, Allen-Worthington KH, Hickman DL, Jonnalagadda M, Newsome JT, Slate AR, Valentine H, Williams AM, Wilkinson M (2020) Review of Rodent Euthanasia Methods. *J Am Assoc Lab Anim Sci* 59:242-253.
- Siebert JR, Conta Steencken A, Osterhout DJ (2014) Chondroitin sulfate proteoglycans in the nervous system: inhibitors to repair. *Biomed Res Int* 2014:845323.
- Soderblom C, Luo X, Blumenthal E, Bray E, Lyapichev K, Ramos J, Krishnan V, Lai-Hsu C, Park KK, Tsoulfas P, Lee JK (2013) Perivascular fibroblasts form the fibrotic scar after contusive spinal cord injury. *J Neurosci* 33:13882-13887.
- Sofroniew MV (2005) Reactive astrocytes in neural repair and protection. *Neuroscientist* 11:400-407.
- Sofroniew MV (2009) Molecular dissection of reactive astrogliosis and glial scar formation. *Trends Neurosci* 32:638-647.
- Sofroniew MV (2018) Dissecting spinal cord regeneration. *Nature* 557:343-350.
- Taylor H, Campbell J, Nobes CD (2017) Ephs and ephrins. *Curr Biol* 27:R90-R95.
- Tran AP, Silver J (2015) Neuroscience. Systemically treating spinal cord injury. *Science* 348:285-286.
- Tran AP, Warren PM, Silver J (2018) The biology of regeneration failure and success after spinal cord injury. *Physiol Rev* 98:881-917.
- Wang ZZ, Wood MD, Mackinnon SE, Sakiyama-Elbert SE (2018) A microfluidic platform to study the effects of GDNF on neuronal axon entrapment. *J Neurosci Methods* 308:183-191.
- Wanner IB, Deik A, Torres M, Rosendahl A, Neary JT, Lemmon VP, Bixby JL (2008) A new in vitro model of the glial scar inhibits axon growth. *Glia* 56:1691-1709.
- Yang IH, Siddique R, Hosmane S, Thakor N, Höke A (2009) Compartmentalized microfluidic culture platform to study mechanism of paclitaxel-induced axonal degeneration. *Exp Neurol* 218:124-128.
- Yang JS, Wei HX, Chen PP, Wu G (2018) Roles of Eph/ephrin bidirectional signaling in central nervous system injury and recovery. *Exp Ther Med* 15:2219-2227.
- Yang K, Park HJ, Han S, Lee J, Ko E, Kim J, Lee JS, Yu JH, Song KY, Cheong E, Cho SR, Chung S, Cho SW (2015) Recapitulation of in vivo-like paracrine signals of human mesenchymal stem cells for functional neuronal differentiation of human neural stem cells in a 3D microfluidic system. *Biomaterials* 63:177-188.
- Zhou JH, Yao M, Wang YS, Li XZ, Zhou Y, Huang W, Chen WY (2021) Spinal cord injury repaired by using nano tissue-engineered spinal cord. *Zhongguo Zuzhi Gongcheng Yanjiu* 25:1550-1554.

P-Reviewer: Goulding S; C-Editor: Zhao M; S-Editors: Yu J, Li CH; L-Editors: Patel B, Yu J, Song LP; T-Editor: Jia Y



Additional Figure 1 Fibroblast/astrocyte coculture without/with scratch treatment.

(A) Photograph of fibroblast/astrocyte coculture for seven days without scratch treatment. Astrocytes and fibroblasts lived in each side separately. There was little crossing between the two types of cells and the cell boundary was clear. (B) Photograph showing fibroblasts were permeating into the astrocytes along the scratched crack 5 days after scratch treatment. (C) Photograph showing 7 days after scratch treatment fibroblasts continued to migrate into the astrocytes, dense cell bands were formed. White line indicates the boundary between the two types of cells. Scale bars: 200 μm.



Additional Figure 2 Co-culture of astrocytes and fibroblasts with different treatments.

(A) Seven days after coculturing fibroblasts and astrocytes there was no cell clusters. (B) Fibroblasts and astrocytes were cocultured for 2 days, added with TGF-β1 at a final concentration of 10 ng/mL (R&D Systems, Inc., Minneapolis, MN, USA) on the 3rd day and finally observed on the 7th day after seeding. Cell clusters (arrows) were formed. (C) Combined treatment of TGF-β1 (on the 3th day after seeding) and RNAi (targeting ephrin-B2) (on the 4th day after seeding), diameter of cell clusters (arrows) decreased. (D) Combined treatment of TGF-β1 (on the 3th day after seeding) and RNAi (targeting EphB2) (on the 4th day after seeding), there was almost no cell clusters although there was still a small amount of cell aggregation. Scale bars: 200 μm. (E) The diameter of cell clusters formed in coculture of astrocytes and fibroblasts with/without TGF-β1 and/or different siRNA. **Data are expressed as mean ± SD (n=12).** The experiments were repeated by three times. * $P < 0.05$, vs. co-culture group; # $P < 0.05$, vs. TGF-β1 group; • $P < 0.05$, vs. TGF-β1 + ephrin-B2 RNAi group (one-way analysis of variance followed by least significant difference test). RNAi: RNA interference; siRNA: small interfering RNA; TGF-β1: transforming growth factor-β1.